Glycobiology vol. 22 no. 1 pp. 12–22, 2012
doi:10.1093/glycob/cwr089
Advance Access publication on July 1, 2011

Glycomic analysis of human mast cells, eosinophils and basophils

Simon J North[2], Stephan von Gunten[3], Aristotelis Antonopoulos[2], Alana Trollope[2], Donald W MacGlashan Jr[3], Jihye Jang-Lee[2], Anne Dell[2], Dean D Metcalfe[4], Arnold S Kirshenbaum[4], Bruce S Bochner[1,3], and Stuart M Haslam[1,2]

[2]Division of Molecular Biosciences, Faculty of Natural Sciences, Imperial College London, London SW7 2AZ, UK; [3]Johns Hopkins Asthma and Allergy Center, 5501 Hopkins Bayview Circle, Rm. 2B.71, Baltimore, MD 21224-6821, USA; and [4]Laboratory of Allergic Diseases, National Institute of Allergy and Infectious Diseases, National Institutes of Health, Bethesda, MD 20892-1881, USA

Received on May 16, 2011; revised on June 15, 2011; accepted on June 27, 2011

In allergic diseases such as asthma, eosinophils, basophils and mast cells, through release of preformed and newly generated mediators, granule proteins and cytokines, are recognized as key effector cells. While their surface protein phenotypes, mediator release profiles, ontogeny, cell trafficking and genomes have been generally explored and compared, there has yet to be any thorough analysis and comparison of their glycomes. Such studies are critical to understand the contribution of carbohydrates to the induction and regulation of allergic inflammatory responses and are now possible using improved technologies for detecting and characterizing cell-derived glycans. We thus report here the application of high-sensitivity mass spectrometric-based glycomics methodologies to the analysis of *N*-linked glycans derived from isolated populations of human mast cells, eosinophils and basophils. The samples were subjected to matrix-assisted laser desorption ionization (MALDI) time-of-flight (TOF) screening analyses and MALDI-TOF/TOF sequencing studies. Results reveal substantive quantities of terminal *N*-acetylglucosamine containing structures in both the eosinophil and the basophil samples, whereas mast cells display greater relative quantities of sialylated terminal epitopes. For the first time, we characterize the cell surface glycan structures of principal allergic effector cells, which by interaction with glycan-binding proteins (e.g. lectins) have the possibility to dictate cellular functions, and might thus have important implications for the pathogenesis of inflammatory and allergic diseases.

[1]To whom correspondence should be addressed: Tel: +1 (410) 550-2101; Fax: +1 (410) 550-1733; e-mail: bbochner@jhmi.edu (B.S.B.) or Tel: +44(0)20 7594 5222; Fax: +44(0)20 7225 0458; e-mail: s.halsam@imperial.ac.uk (S.M.H.)

Keywords: basophil / eosinophil / glycomics / mass spectrometry / mast cell

Introduction

Eosinophils, basophils and mast cells comprise the triumvirate of principal allergic effector cells. Each cell type has its own bone marrow differentiation paradigm, as well as distinct, yet often overlapping pathways regulating their development, migration, activation, survival and death (Bochner and Schleimer 2001). Much of what is known about the biologic contributions of these cell types to allergic and other forms of inflammation stems from extensive efforts to characterize their release of preformed and newly generated mediators, granule proteins and cytokines. It has also been revealing to compare and contrast the capabilities and characteristics of these cells at the protein and gene levels (Valent 1994; Agis et al. 1996; Miyazaki et al. 1997; Nakajima et al. 2001).

The mammalian glycome, namely the entire complement of carbohydrates in or on a cell, is encoded by a series of post-translational modifications made to proteins and lipids. Hundreds of enzymes control these steps, which are primarily carried out within the Golgi of each cell. These glycans appear to have multiple and overlapping functions. They are recognized by glycan-binding proteins with lectin activity on apposing cells, and such glycan-ligand interactions mediate many biologic activities including recognition of pathogens and induction of intracellular signaling pathways. Although information on the biological roles of glycan-binding proteins continues to evolve, challenges remain in detecting and quantifying existing and novel cellular glycans.

Advances over the last decade in mass spectrometric techniques, most notably the development and increased utilization of the MALDI-TOF/TOF mass spectrometer, have driven a period of steady progress in the analysis of glycan populations derived from biological samples previously considered too complex or low in abundance to provide meaningful data. The comparative improvements provisioned by such techniques are exemplified by a recent glycomic reassessment of human neutrophil isolates (Babu et al. 2009). Dramatic improvements in upper mass range and signal-to-noise ratios, in addition to substantive increases in sensitivity and resolution allowed the characterization of an expanded population of both protein *N*- and *O*-linked glycans. Coupled with the ability to fragment glycan molecular ions and produce informative structural data at masses up to 6000 Da, these and similar related techniques

(such as electron transfer dissociation and electron capture dissociation; Perdivara et al. 2009) are now allowing the glycomic characterization of immune cell populations, even those with relatively limited abundance.

Indeed, the primary focus of one of the major international glycobiology consortia, the Consortium for Functional Glycomics (CFG), is the analysis of mammalian immune cell populations. To date, structural profiling work has been completed on a number of important components, including neutrophils (Babu et al. 2009), dendritic cells (Bax et al. 2007), monocytes, natural killer cells and T- and B-lymphocytes as well as erythrocytes. Data from all work are freely available in the CFG databases (http://www.functionalglycomics.org/glycomics/publicdata/glycoprofiling-new.jsp).

This paper represents the first structural analysis of *N*-glycans derived from samples of human basophils, eosinophils and mast cells. The eosinophil and basophil samples share a high level of heavily truncated structures with limited levels of sialylated termini, while the mast cells conversely exhibit a relatively high abundance of terminal sialic acid.

Results

Glycomics screening strategy

In order to produce isolated pools of *N*-linked glycans derived from each of the investigated cell types (human basophils, eosinophils and mast cells), each sample was sonicated, reduced, carboxymethylated and proteolytically digested with trypsin to produce short peptides and glycopeptides amenable to enzymatic deglycosylation. *N*-Linked glycan release was then achieved by means of treatment of these tryptic fragments with peptide *N*-glycosidase F (PNGase F). Once purified, the pool of *N*-glycans was derivatized by means of chemical permethylation in order to enhance the sensitivity of mass spectrometric detection and to assist predictable fragmentation when subjected to tandem mass spectrometry (MS)/MS analysis. MALDI-TOF-MS profiling was utilized in order to produce a fingerprint of the derivatized *N*-glycans derived from each original cell sample. These profiles consist of singly charged sodiated molecular ions ($[M + Na]^+$) that are putatively identified by means of a combination of compositional analysis and knowledge of available biosynthetic pathways. These tentative assignments are then reinforced by supplementary experiments utilizing tandem MS/MS analyses and gas chromatography (GC)-MS linkage studies, which are variously capable of confirming the presence of structural features such as antennal arrangements, terminal moieties and core modifications such as fucosylation or the presence of bisecting *N*-acetylglucosamine (GlcNAc) residues. The assignment of both glycan MS and MS/MS spectra are assisted by the application of the glycoinformatic tools Cartoonist and GlycoWorkbench (Goldberg et al. 2005; Ceroni et al. 2008).

Though mass spectrometric analyses of this type are not fully quantitative, recent studies have established that relative quantitation based on the signal strength of permethylated glycans analyzed by MALDI-TOF MS is indeed both possible and accurate, especially when comparisons are carried out among related species across small mass ranges (Wada et al. 2007).

Basophils

Samples of basophils were subjected to the glycomics screening strategy, as outlined in the glycomics screening strategy section. The PNGase F released *N*-linked glycans were derivatized via permethylation and analyzed by MALDI-TOF-MS analysis. The results of a typical analysis are displayed in Figure 1A. Complete compositional assignments can be found in Table I.

The *N*-glycan spectrum of human basophils contains a full complement of high-mannose (Man) type structures (*m/z* 1579.8, 1783.9, 1988.0, 2192.1 and 2396.2), as well as a series of complex type glycans comprising a mixture of bi-, tri- and tetra-antennary structures. These are mostly core-fucosylated, with a relatively low level of *N*-acetylneuraminic acid (NeuAc) terminal residues ($n = 1–2$); and some evidence for low-abundance antennal fucosylation and simple hybrid glycans.

The spectrum is characterized by the presence of a high abundance of unsubstituted terminal GlcNAc residues. These part-processed structures are present throughout the spectrum in significant quantities and are interspersed with structures bearing a bisecting GlcNAc residue, an observation verified by significant levels of 3,4,6-linked Man identified in GC-MS linkage analyses (data not shown). The most prominent peak in the basophil sample at *m/z* 1835.9 corresponds to a glycan composition of $Fuc_1Hex_3HexNAc_4$, consistent with a core-fucosylated part-processed structure bearing a pair of exposed GlcNAc residues. MALDI-TOF/TOF MS/MS fragmentation analysis of this molecular ion (Figure 2) confirms this as the most likely arrangement of the individual residues. The level at which this and other truncated structures are present in the sample can be assessed by evaluation of the levels at which similar glycans are observed in the mass spectrum, in this case the truncated core-fucosylated structure with and without galactose (Gal) extensions on the putative antennae. Comparison of the relative intensities of three related species at *m/z* 1835.9, 2040.0 and 2244.1 (corresponding to compositions of $Fuc_1Hex_3HexNAc_4$, $Fuc_1Hex_4HexNAc_4$ and $Fuc_1Hex_5HexNAc_4$, respectively) shows a ratio of relative intensities of 8:4:1, indicating that the non-substituted structure is approximately twice as abundant as its singly galactosylated form.

Eosinophils

Approximately 10×10^7 human eosinophils isolated from allergic donors were subjected to the glycomics methodology described in the glycomics screening strategy section. The mass spectrum acquired from a typical sample of released, permethylated *N*-glycans is shown in Figure 1B, with the complete annotation of the spectrum presented in Table I.

The eosinophil samples produce a very similar glycomics profile to that of the basophils. The full complement of high-Man *N*-glycans are present (*m/z* 1579.8, 1783.9, 1988.0, 2192.1 and 2396.2) and a number of complex glycans can be identified, with antennal arrangements consistent with bi-, tri- and tetra-antennary forms. Sialylation is a relatively low-abundance terminal modification, though slightly more prominent than in the comparable basophil sample ($n = 1–3$). Some low-level antennal fucosylation is also observed, together with limited amounts of simple hybrid structures.

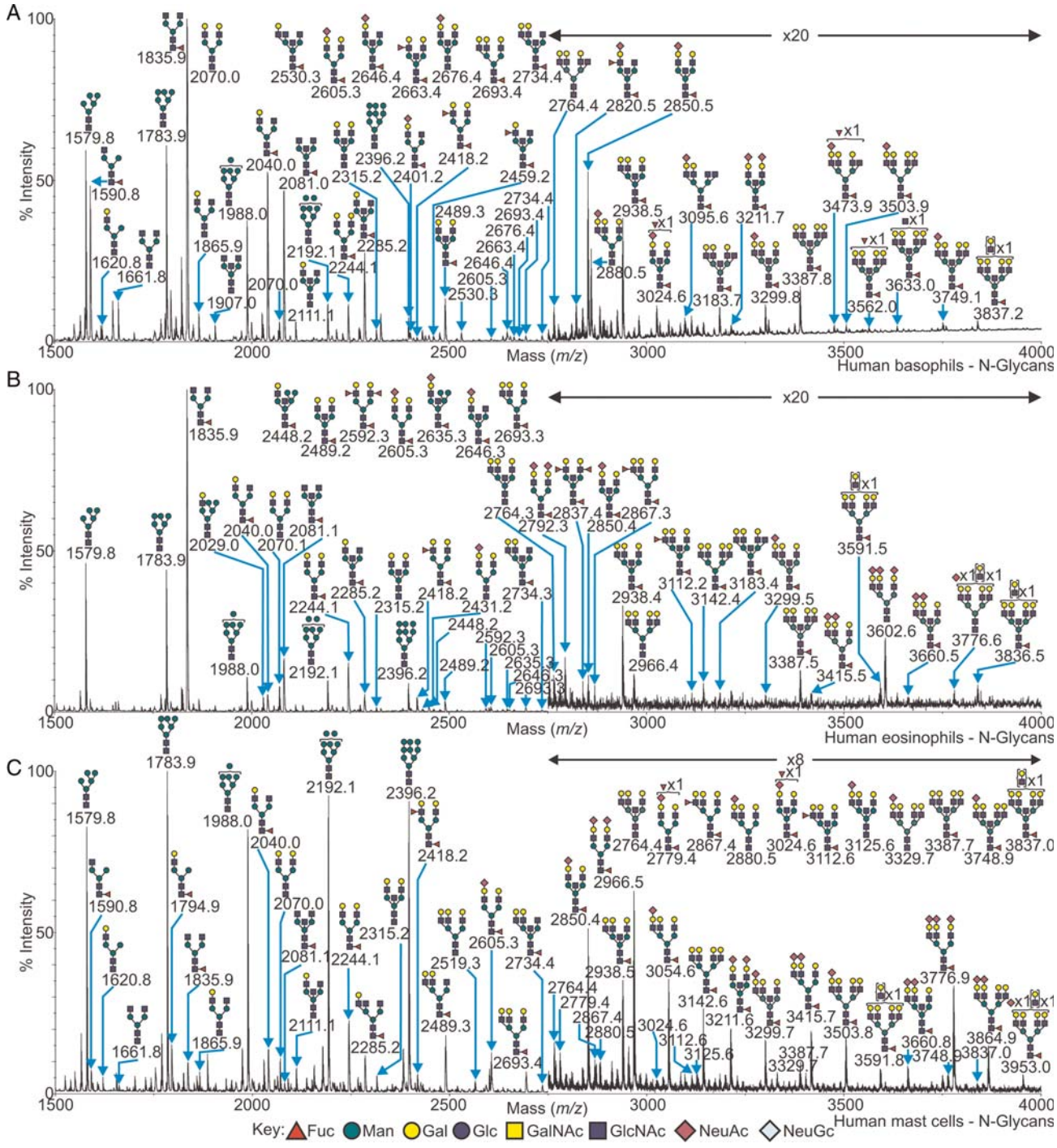

Fig. 1. MALDI-TOF MS profiles of the permethylated *N*-linked glycans from human basophils (**A**), eosinophils (**B**) and mast cells (**C**). Major peaks are annotated with their proposed carbohydrate structure, according to the symbolic nomenclature adopted by the CFG (Varki et al. 2009). For complete annotations of the spectra, see Table I. All molecular ions are present in singly charged sodiated form ($[M+Na]^+$).

The distinctive feature of the eosinophil spectra, in similar fashion to the basophils, is a remarkable level of truncated or unsubstituted part-processed glycans. The base peak of the spectrum at *m/z* 1835.9 corresponds to the same core-fucosylated part-processed structure bearing a pair of exposed GlcNAc residues that was observed in the basophils and was similarly confirmed via MS/MS analyses (data not shown). Comparison of the intensities of the related peaks at *m/z* 1835.9, 2040.0 and 2244.1 in the eosinophil sample (corresponding to compositions of $Fuc_1Hex_3HexNAc_4$, $Fuc_1Hex_4HexNAc_4$ and $Fuc_1Hex_5HexNAc_4$, respectively) establishes a ratio of relative intensities of approximately 17:1:3, indicating that the unsubstituted structure is some 17 times more abundant than the singly galactosylated form.

Table I. Compositional assignments of singly charged sodiated molecular ions, $[M+Na]^+$, observed in the MALDI-MS spectra of permethylated *N*-glycans from human basophils, eosinophils, mast cells and LAD2 cells

Molecular assignment	Basophils observed mass (*m*/*z*)	Eosinophils observed mass (*m*/*z*)	Mast cells observed mass (*m*/*z*)	LAD2 cells observed mass (*m*/*z*)
$Hex_5HexNAc_2$	1579.8	1579.8	1579.8	1579.8
$Fuc_1Hex_3HexNAc_3$	1590.8	1590.8	1590.8	1590.8
$Hex_4HexNAc_3$	1620.8	1620.8	1620.8	—
$Hex_3HexNAc_4$	1661.8	1661.8	1661.8	—
$Hex_6HexNAc_2$	1783.9	1783.9	1783.9	1783.9
$Fuc_1Hex_4HexNAc_3$	—	1794.9	1794.9	1794.9
$Hex_5HexNAc_3$	—	1824.9	1824.9	1824.9
$Fuc_1Hex_3HexNAc_4$	1835.9	1835.9	1835.9	1835.9
$Hex_4HexNAc_4$	1865.9	1866.0	1865.9	—
$Hex_3HexNAc_5$	1907.0	1907.0	1905.9	—
$Hex_7HexNAc_2$	1988.0	1988.0	1988.0	1988.0
$Fuc_1Hex_5HexNAc_3$	—	1999.0	1999.0	1999.0
$Hex_6HexNAc_3$	—	2029.0	2029.0	2029.0
$Fuc_1Hex_4HexNAc_4$	2040.0	2040.0	2040.0	2040.0
$Hex_5HexNAc_4$	2070.0	2070.1	2070.0	2070.0
$Fuc_1Hex_3HexNAc_5$	2081.0	2081.1	2081.1	2082.0
$Hex_4HexNAc_5$	2111.1	2111.1	2111.1	—
$NeuAc_1Fuc_1Hex_4HexNAc_3$	—	—	2156.1	2156.1
$Hex_8HexNAc_2$	2192.1	2192.1	2192.1	2192.1
$Fuc_1Hex_6HexNAc_3$	—	2203.0	2203.1	2203.1
$Fuc_2Hex_4HexNAc_4$	2214.1	2214.1	2214.1	—
$Fuc_1Hex_5HexNAc_4$	2244.1	2244.1	2244.1	2244.1
$Hex_6HexNAc_4$	—	2274.1	2274.1	2274.2
$Fuc_1Hex_4HexNAc_5$	2285.2	2285.2	2285.2	2286.1
$Hex_5HexNAc_5$	2315.2	2315.2	2315.2	—
$Fuc_1Hex_3HexNAc_6$	2326.2	2326.2	2326.2	—
$NeuAc_1Fuc_1Hex_5HexNAc_3$	—	—	—	2360.2
$NeuAc_1Hex_6HexNAc_3$	—	—	—	2390.2
$Hex_9HexNAc_2$	2396.2	2396.2	2396.2	2396.2
$NeuAc_1Fuc_1Hex_4HexNAc_4$	2401.2	2401.2	—	—
$Fuc_2Hex_5HexNAc_4$	2418.2	2418.2	2418.2	2418.2
$NeuAc_1Hex_5HexNAc_4$	2431.2	2431.2	2431.2	2431.2
$Fuc_1Hex_6HexNAc_4$	2448.2	2448.2	2448.2	2448.2
$Fuc_2Hex_4HexNAc_5$	2459.2	2459.2	2459.3	—
$Fuc_1Hex_5HexNAc_5$	2489.3	2489.2	2489.3	2489.3
$Hex_6HexNAc_5$	2519.3	2519.2	2519.3	2519.3
$Fuc_1Hex_4HexNAc_6$	2530.3	2530.3	2530.3	—
$Hex_5HexNAc_6$	2560.3	2560.3	2560.3	—
$NeuAc_1Fuc_1Hex_6HexNAc_3$	—	—	—	2564.2
$NeuAc_1Fuc_2Hex_4HexNAc_4$	2575.3	—	—	—
$Fuc_3Hex_5HexNAc_4$	—	2592.3	—	2592.3
$Hex_{10}HexNAc_2$	—	2600.3	2600.3	2600.4
$NeuAc_1Fuc_1Hex_5HexNAc_4$	2605.3	2605.3	2605.3	2605.3
$NeuAc_1Hex_6HexNAc_4$	2635.3	2635.3	2635.3	2635.3
$NeuAc_1Fuc_1Hex_4HexNAc_5$	2646.4	2646.3	2646.3	—
$Fuc_1Hex_7HexNAc_4$	—	2652.3	—	—
$Fuc_2Hex_5HexNAc_5$	2663.4	2663.3	2663.3	—
$NeuAc_1Hex_5HexNAc_5$	2676.4	—	2676.4	—
$Fuc_1Hex_6HexNAc_5$	2693.4	2693.3	2693.4	2693.4
$Fuc_1Hex_5HexNAc_6$	2734.4	2734.3	2734.4	—
$Hex_6HexNAc_6$	2764.4	2764.3	2764.4	—
$Fuc_1Hex_4HexNAc_7$	2775.5	—	—	—
$NeuAc_1Fuc_2Hex_5HexNAc_4$	—	2779.4	2779.4	2779.4
$NeuAc_2Hex_5HexNAc_4$	—	2792.3	—	2792.3
$NeuAc_1Fuc_1Hex_6HexNAc_4$	—	—	—	2809.4
$NeuAc_1Fuc_2Hex_4HexNAc_5$	2820.5	—	—	—
$Fuc_3Hex_5HexNAc_5$	—	2837.4	—	—
$NeuAc_1Fuc_1Hex_5HexNAc_5$	2850.5	2850.4	2850.4	2850.4
$Fuc_2Hex_6HexNAc_5$	—	2867.3	2867.4	2867.4
$NeuAc_1Hex_6HexNAc_5$	2880.5	—	2880.5	2880.4
$NeuAc_1Fuc_1Hex_4HexNAc_6$	2891.5	—	—	—
$Fuc_2Hex_5HexNAc_6$	2908.5	—	2908.5	—
$Fuc_1Hex_6HexNAc_6$	2938.5	2938.4	2938.5	2938.5
$NeuAc_2Fuc_1Hex_5HexNAc_4$	—	2966.4	2966.5	2966.5
$Fuc_1Hex_5HexNAc_7$	2979.6	—	—	—
$NeuAc_1Fuc_2Hex_5HexNAc_5$	3024.6	—	3024.6	—
$NeuAc_1Fuc_1Hex_6HexNAc_5$	3054.6	—	3054.5	3054.5
$NeuAc_1Hex_7HexNAc_5$	3084.6	—	3084.6	3084.6
$NeuAc_1Fuc_1Hex_5HexNAc_6$	3095.6	—	3095.6	—
$Fuc_2Hex_6HexNAc_6$	3112.6	3112.2	3112.6	—
$NeuAc_1Hex_6HexNAc_6$	3125.6	—	3125.6	3125.5
$Fuc_1Hex_7HexNAc_6$	3142.7	3142.4	3142.6	3142.5
$Fuc_1Hex_6HexNAc_7$	3183.7	3183.4	3183.6	—
$NeuAc_2Fuc_1Hex_5HexNAc_5$	3211.7	3211.9	3211.6	3211.6
$NeuAc_1Fuc_1Hex_6HexNAc_6$	3299.8	3299.5	3299.7	3299.6
$Fuc_2Hex_7HexNAc_6$	—	—	—	3316.6
$NeuAc_1Hex_7HexNAc_6$	3329.8	—	3329.7	3329.6
$NeuAc_1Hex_7HexNAc_6$	—	—	—	3329.6
$Fuc_1Hex_7HexNAc_7$	3387.8	3387.5	3387.7	—
$NeuAc_2Fuc_1Hex_6HexNAc_5$	—	3415.5	3415.7	3415.7
$NeuAc_1Fuc_2Hex_6HexNAc_6$	3473.9	—	—	3473.7
$NeuAc_1Fuc_1Hex_7HexNAc_6$	3503.9	—	3503.8	3503.7
$Fuc_2Hex_7HexNAc_7$	3562.0	—	—	—
$Fuc_1Hex_8HexNAc_7$	—	3591.5	3591.8	3591.7
$NeuAc_3Hex_6HexNAc_5$	—	3602.6	—	3602.9
$Fuc_1Hex_7HexNAc_8$	3633.0	3632.5	—	—
$NeuAc_2Fuc_1Hex_6HexNAc_6$	—	3660.5	3660.8	3660.7
$NeuAc_1Fuc_2Hex_7HexNAc_6$	—	—	—	3677.7
$NeuAc_2Hex_7HexNAc_6$	—	—	—	3690.8
$NeuAc_1Fuc_1Hex_7HexNAc_7$	3749.1	—	3748.9	—
$Fuc_2Hex_8HexNAc_7$	—	—	—	3765.8
$NeuAc_3Fuc_1Hex_6HexNAc_5$	—	3776.6	3776.9	3776.8
$Fuc_1Hex_8HexNAc_8$	3837.2	3836.5	3837.0	—
$NeuAc_2Fuc_1Hex_7HexNAc_6$	—	—	3864.9	3864.8
$NeuAc_1Fuc_1Hex_8HexNAc_7$	—	—	3953.0	3952.8
$NeuAc_2Fuc_2Hex_7HexNAc_6$	—	—	—	4038.9
$Fuc_1Hex_9HexNAc_8$	—	—	4041.1	—
$NeuAc_3Hex_7HexNAc_6$	—	—	—	4051.8
$NeuAc_2Fuc_1Hex_7HexNAc_7$	—	—	4109.9	—
$NeuAc_1Fuc_2Hex_8HexNAc_7$	—	—	—	4126.9
$NeuAc_4Fuc_1Hex_6HexNAc_5$	—	—	4138.1	—
$NeuAc_3Fuc_1Hex_7HexNAc_6$	—	4225.7	4226.1	4226.0
$Fuc_1Hex_9HexNAc_9$	—	4285.5	—	—
$NeuAc_2Fuc_1Hex_8HexNAc_7$	—	—	4314.2	4314.0
$NeuAc_1Fuc_1Hex_9HexNAc_8$	—	—	4402.2	4402.1
$NeuAc_3Fuc_1Hex_7HexNAc_7$	—	—	4471.4	—
$NeuAc_2Fuc_2Hex_8HexNAc_7$	—	—	—	4488.1
$NeuAc_4Fuc_1Hex_7HexNAc_6$	—	—	4587.2	4587.2
$NeuAc_3Fuc_1Hex_8HexNAc_7$	—	—	4675.3	4675.1
$NeuAc_2Fuc_1Hex_9HexNAc_8$	—	—	4763.8	4763.3
$NeuAc_3Fuc_2Hex_8HexNAc_7$	—	—	—	4849.2
$NeuAc_4Fuc_1Hex_8HexNAc_7$	—	—	5036.4	5036.1
$NeuAc_3Fuc_1Hex_9HexNAc_8$	—	—	5124.3	5125.1
$NeuAc_4Fuc_1Hex_9HexNAc_8$	—	—	5485.5	5485.2

Bisecting GlcNAc is again a common structural feature among the *N*-glycans derived from the eosinophil samples, though at a slightly lower relative level when compared with that of the basophils.

Mast cells

Samples of human mast cells containing $\sim 15 \times 10^6$ cells were taken through the glycomics screening procedure as described. Isolated *N*-glycans were chemically modified into their permethyl derivatives and analyzed by MALDI-TOF and

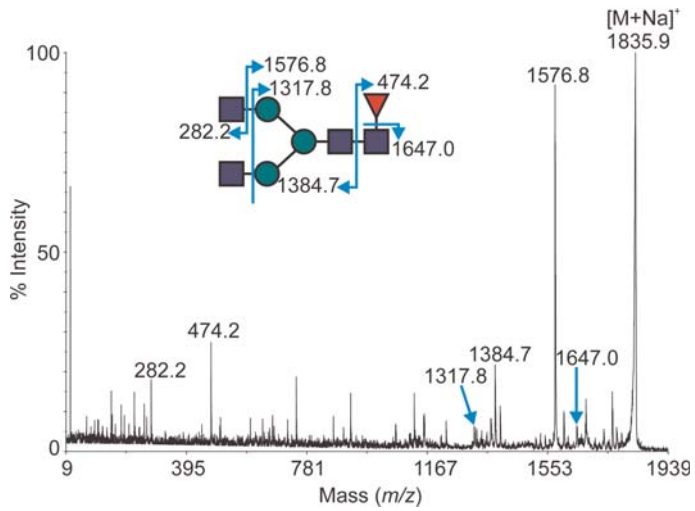

Fig. 2. MALDI-TOF/TOF MS/MS fragmentation spectrum of the $[M + Na]^+$ molecular ion observed at *m/z* 1835.9 from the permethylated *N*-glycan pool derived from the human basophil cell sample (Figure 1A). The peak is by far the most abundant ion in the spectrum and corresponds to a monosaccharide composition of $Fuc_1Hex_3HexNAc_4$. Assignments of the product ions are indicated.

MALDI-TOF/TOF MS, with the annotated results displayed in Figure 1C. Full assignments of all of the observed molecular ions can be found in Table I.

The high-Man family of glycan structures is present (at *m/z* 1579.8, 1783.9, 1988.0, 2192.1 and 2396.2) together with a low level of simple hybrid structures. The majority of the high-abundance signals among *N*-glycans derived from mast cells are of the complex type, comprising bi-, tri- and tetra-antennary structures, the vast majority of which are core-fucosylated. Bisecting GlcNAc is also a common structural feature, with some limited antennal fucosylation also present. There is a significant level of terminal NeuAc sialylation present within the *N*-glycan profile of the mast cells, with the majority of abundant peaks bearing between one and four sialic acid residues. This is especially evident in the higher mass region of the spectrum, with the larger structures being observed almost exclusively with high levels of sialylation. Much larger structures than those observed in either the basophil or the eosinophil samples are also evident, with up to three poly-*N*-acetyllactosamine extensions (Galβ1-4GlcNAc β1-3-) observed.

Significantly, the mast cell sample displays only small amounts of the truncation/part processing that is abundant among the *N*-glycans of both the basophils and the eosinophils. Making the same comparison between the related peaks at *m/z* 1835.9, 2040.0 and 2244.1 in the mast cell sample (corresponding to compositions of $Fuc_1Hex_3HexNAc_4$, $Fuc_1Hex_4HexNAc_4$ and $Fuc_1Hex_5HexNAc_4$, respectively) yields a ratio of relative intensities of approximately 1:1:2, showing that the abundance of a typical unsubstituted putative antenna is approximately the same as that of a galactosylated one.

LAD2 cells

N- and *O*-linked glycans were isolated from cultured human leukocyte adhesion deficiency 2 (LAD2) cells utilizing the glycomics methodology detailed in the glycomics screening strategy section. The permethylated derivatives of these glycans were then analyzed by MALDI-TOF and MALDI-TOF/TOF MS, with the annotated results displayed in Figure 3 (*N*-glycans) and Figure 4 (*O*-glycans). Full assignments of all of the observed molecular ions can be found in Table I.

In a similar fashion to the *N*-linked glycan pools derived from the other cell types in this study, the LAD2 cell line produces a full range of high-Man glycans (observed at *m/z* 1580.2, 1784.3, 1988.4, 2192.5 and 2396.5) together with some low abundance hybrid-type structures. Prevalent among the mid to high-mass regions are a series of complex glycans, bearing two, three and four antennae, most of which are fucosylated at the core and it is of note that there is a particularly significant amount of tetra-antennary glycans. Some evidence for bisecting GlcNAc is observed, but together with antennal fucosylation, this structural modification appears to be minimal. Sialylation is abundant, with the majority of the complex *N*-glycans bearing between one and three NeuAc terminal epitopes on their antennae. LacNAc (Galβ1-4GlcNAc) extension of antenna is also common, with the largest glycans possessing at least three poly-*N*-acetyllactosamine extensions.

Significantly less truncated structures are observed among the *N*-glycan population of the LAD2 cell line when compared with similar samples from the other immune cells studied here. The truncated core-fucosylated structure and the singly galactosylated glycan (corresponding to compositions of $Fuc_1Hex_3HexNAc_4$ and $Fuc_1Hex_4HexNAc_4$) prominent in the other samples are both present in vanishingly small quantities when compared with the di-galactosylated form at *m/z* 2245.5, which is present in a quantity of ~10 times that of the others.

The advantages of studying a cell line such as a stem cell factor (SCF) dependent human mast cell line like LAD2, as opposed to cell isolates, are readily apparent in the number of additional experiments that can be effectively performed within the glyco-analysis framework. High-quality data from chemically released *O*-glycans were additionally obtained and a typical profile from a subsequent MALDI-TOF analysis of the permethyl derivatives is shown in Figure 4. The vast majority of the *O*-glycans produced by the LAD2 cells are of core-1 type, with high levels of sialylation by NeuAc.

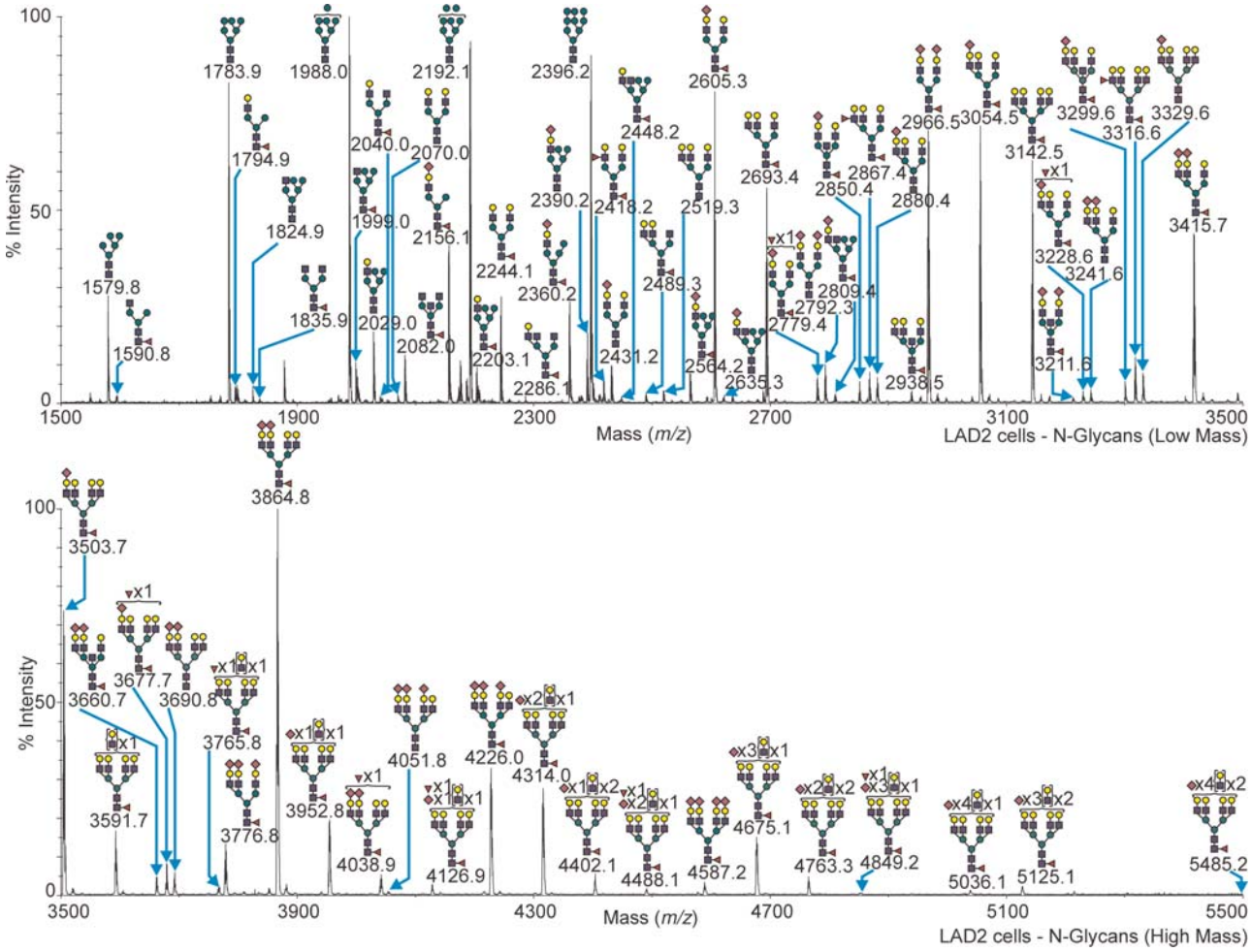

Fig. 3. MALDI-TOF MS profile of the permethylated *N*-linked glycans from human LAD2 mast cells. Major peaks are annotated with their proposed carbohydrate structure, according to the symbolic nomenclature adopted by the CFG (Varki et al. 2009). For complete annotations of the spectra, see Table I. All molecular ions are present in singly charged sodiated form ($[M + Na]^+$).

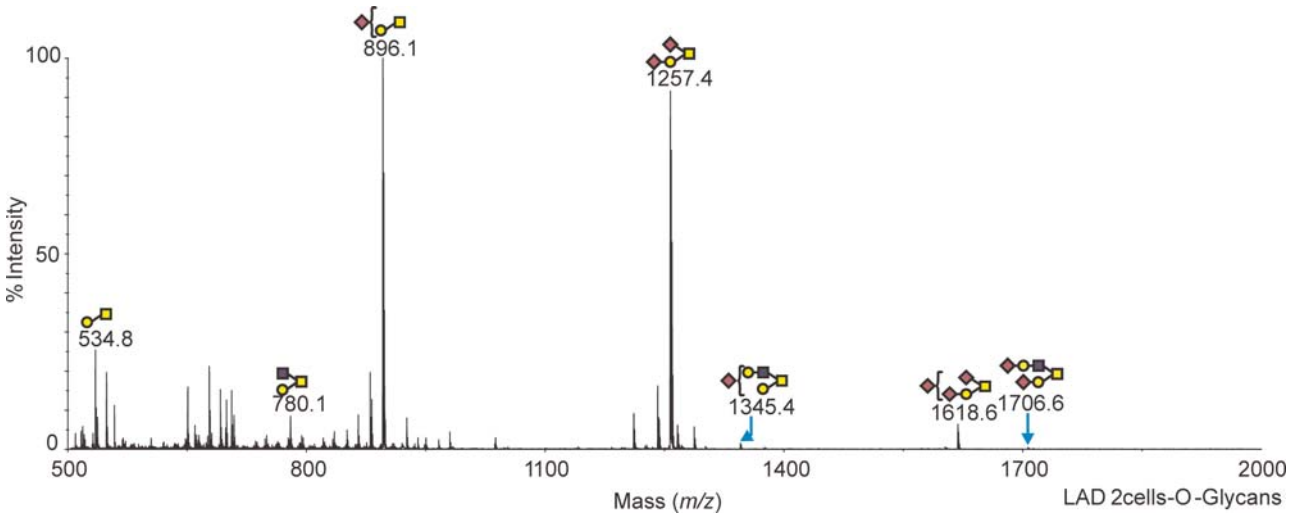

Fig. 4. MALDI-TOF MS profile of the permethylated *O*-linked glycans from human LAD2 mast cells. Peaks are annotated with their proposed carbohydrate structure, according to the symbolic nomenclature adopted by the CFG (Varki et al. 2009). For complete annotations of the spectrum, see Table II. All molecular ions are present in a singly charged sodiated form ($[M + Na]^+$).

Table II. Compositional assignments of singly charged sodiated molecular ions, $[M+Na]^+$, observed in the MALDI-MS spectra of permethylated *O*-glycans from human basophils, eosinophils, mast cells and LAD2 cells

Molecular assignment	Basophils observed mass (*m/z*)	Eosinophils observed mass (*m/z*)	Mast cells observed mass (*m/z*)	LAD2 cells observed mass (*m/z*)
$Hex_1HexNAc_1$-itol	534.4	—	534.3	534.8
$Hex_1HexNAc_2$-itol	780.6	—	—	780.1
$NeuAc_1Hex_1HexNAc_2$-itol	896.2	—	—	896.1
$NeuAc_2Hex_1HexNAc_2$-itol	—	—	—	1257.4
$NeuAc_1Hex_2HexNAc_2$-itol	—	—	—	1345.4
$NeuAc_3Hex_1HexNAc_2$-itol	—	—	—	1618.6
$NeuAc_2Hex_2HexNAc_2$-itol	—	—	—	1706.6

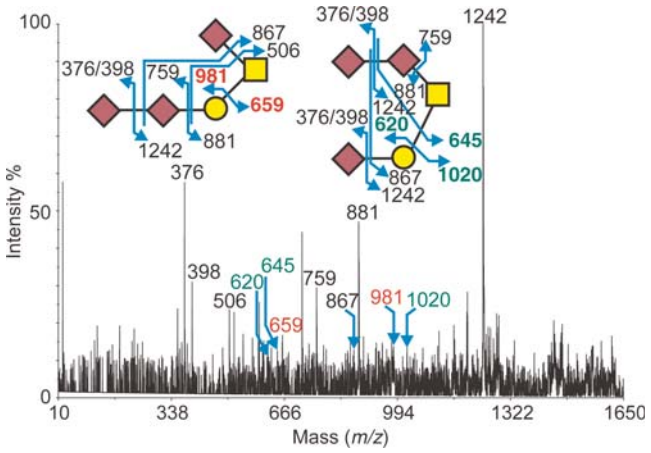

Fig. 5. MALDI-TOF/TOF MS/MS fragmentation spectrum of the $[M + Na]^+$ molecular ion observed at *m/z* 1618.6 from the permethylated *O*-glycan derived from the human LAD2 mast cells (Figure 4). The peak corresponds to a monosaccharide composition of $NeuAc_3Hex_1HexNAc_1$. Assignments of the product ions are indicated.

Abundant peaks observed at *m/z* 896.1 and 1257.4 (corresponding to $NeuAc_1Hex_1HexNAc_1$-itol and $NeuAc_2Hex_1HexNAc_1$-itol, respectively) dominate the spectrum, though low levels of similarly sialylated core 2 structures are also observed. Of note is the structure at *m/z* 1618.6 whose composition is consistent with a tri-sialylated core 1 *O*-glycan. This was confirmed by subsequent MALDI-TOF/TOF MS/MS fragmentation analysis of this molecular ion (Figure 5). Key fragment ions at *m/z* 981/659 and 620/1020 indicate two possible structural isomers in which the NeuAcα2-8NeuAc di-sialylated motif can be linked to either the Gal or *N*-acetylgalactosamine of the core 1 *O*-glycan.

Discussion

This paper describes the first detailed glycomic analysis of human eosinophils, basophils and mast cells that play important roles in maintaining homeostasis and in the induction and perpetuation of allergic and other forms of inflammation. In addition, human LAD2 cultured mast cells were glycomically characterized. All the analyzed cells displayed both high-Man and complex-type *N*-glycans. One of the most striking features of the data is that both eosinophils and basophils contain a large proportion of part-processed *N*-glycans which therefore display large quantities of terminal β-linked GlcNAc residues. This is clearly illustrated by the fact that in both species the most abundant *N*-glycan is a bi-antennary structure with two terminal non-extended GlcNAc residues (Figures 1 and 2). This dramatically contrasts to culture-derived human mast cells (and LAD2 mast cells) which display more highly processed *N*-glycans with sialylated and fucosylated multi-antennary structures and other immune cells, such as human neutrophils, which have been similarly glycomically characterized. These possess the most complex *N*-glycome to date with bi-, tri- and tetra-antennary structures, capped with one, two, three or four sialic acid residues with a high degree of fucosylation as well as prevalent poly-LacNAc extensions (Babu et al. 2009).

As the glycans characterized in this study will be located on the cells primary interface with their external environment, the cell surface, they must be involved in interactions which dictate cellular functions. Such interactions will involve the recognition of a specific glycan structure by a specific lectin. Previous characterization of these cells by lectin-binding studies has been limited. Lectin histochemistry of human mast cell populations demonstrated binding with concanavalin A (ConA), pisum sativum agglutinin (PSA), lens culimaris agglutinin (LCA), phaseolus vulgaris lectin E (e-PHA), phaseolus vulgaris lectin L (l-PHA) and wheat germ agglutinin (WGA), the specificities of which are all consistent with the proposed glycan structures we present (Roberts et al. 1990). As stated above, both human eosinophils and basophils will present a large amount of terminal β-linked GlcNAc residues for specific lectin interactions. The C-type lectin LSECtin, which is predominantly expressed on the liver and lymph node sinusoidal endothelial cells, has been demonstrated to bind with high selectivity to *N*-glycans displaying terminal GlcNAcβ1-2Man structures. Indeed, the calculated inhibition constant of 3.5 μM for the GlcNAcβ1-2Man disaccharide indicates one of the highest relative affinities of any C-type lectin (Powlesland et al. 2008). *N*-Glycans expressing the GlcNAcβ1-2Man disaccharide structures such as *m/z* 1835.9 are highly abundant in both basophils and eosinophils (Figures 1 and 2). Within the liver LSECtin has been demonstrated to have an immunomodulatory function inhibiting T-cell responses. Also when recombinant LSECtin was administered intravenously, it significantly reduces acute liver inflammatory injury (Tang et al. 2009). Such immunomodulatory and anti-inflammatory function could extend beyond the liver, as LSECtin has also been demonstrated to be expressed by human peripheral blood and thymic dendritic cells and monocyte-derived macrophages (Dominguez-Soto et al. 2007). Indeed, LSECtin expressed on immune-related cells has been demonstrated to mediate intracellular interactions with partner cells via recognition of the same terminal β-linked GlcNAc rich *N*-glycans as we have demonstrated to be present on both human eosinophils and basophils (Yabe et al. 2010).

A second potential binding partner for the GlcNAc rich eosinophils and basophils cell surface is the protein YKL-40. This is a chitinase-like protein which lacks hydrolytic enzymatic activity but retains the ability to bind to β-GlcNAc

(Lee and Elias 2010). Increased levels of YKL-40 have been linked with a wide range of human diseases, particularly those associate with inflammation, allergy and tissue remodeling, as illustrated by the fact that asthmatic patents show a significantly higher level of YKL-40 than non-asthmatic controls and that asthma severity also correlates with YKL-40 levels (Ober and Chupp 2009). In addition, YKL-40 levels have also been linked to cigarette smoke induced inflammation and emphysema (Matsuura et al. 2011). Studies from BRP-39 (the mouse homolog of YKL-40)$^{-/-}$ KO mice demonstrated a reduced antigen-induced Th2 inflammatory reaction and reduced death receptor-mediated eosinophil cell apoptosis (Lee et al. 2009). As yet, no cell surface ligand for YKL-40 has been identified. It is enticing to hypothesize that YKL-40 is not binding to a cell surface protein but to the GlcNAc rich *N*-glycans which we have characterized in this study.

Although both eosinophils and basophils contain a large proportion of part-processed *N*-glycans, they do also express more highly processed sialylated glycans. Such extensively processed sialylated glycans are much more highly expressed on both human mast cells and the LAD2 human mast cells. Sialylated glycans can be recognized by siglecs (sialic acid-binding immunoglobulin-like lectins) that are predominantly expressed by immune cells where, via their cytoplasmic immunoreceptor tyrosine-based inhibitory motif (ITIM) and ITIM-like domains, they regulate cell signaling. Siglecs can recognize sialylated glycans both in the context of *cis* (same cell) and *trans* (adjacent cell) interactions (Crocker et al. 2007). Of the 14 currently identified siglecs, mast cells and basophils have been demonstrated to express siglec-3, -5, -6, -8 and -14, whereas eosinophils express siglec-8 and -10 (O'Reilly and Paulson 2009). It is noteworthy that both siglec-5 and -14 have a preferred specificity for the NeuAcα2-8NeuAc di-sialylated motif that we identified on the human mast cell line LAD2 *O*-glycans (Figures 4 and 5). This remains a relatively rare glycan sequence being limited to a small number of blood-associated glycoproteins such as immunoglobulins, MUC-1, α2-macroglobulin, vitronectin, glycophorin, plasminogen and von Willebrand factor (Fukuda et al. 1987; Yasukawa et al. 2006; Canis et al. 2010). The structure has also been described on the *O*-glycans of human natural killer cells where it is thought to interact with siglec-7 regulating cellular activation (Avril et al. 2006).

In summary, we report here that the application of high-sensitivity mass spectrometric-based glycomics (MALDI-TOF/TOF sequencing) to compare and contrast human eosinophil, basophil and mast cell glycomes. Results reveal substantive quantities of terminal GlcNAc-containing structures in both the eosinophil and basophil samples, while mast cells display greater relative quantities of sialylated terminal epitopes. These novel findings may have important implications for the involvement and interaction of eosinophils, basophils and mast cells during inflammation and allergic diseases.

Materials and methods

Cell purification and culture methods

Basophils. Residual cell byproducts of normal donors undergoing plateletpheresis were enriched in basophils using a combination of Percoll density gradients and countercurrent-flow elutriation and negative selection using columns from Miltenyi Biotec (Auburn, CA) and Stem Cell basophil isolation reagents (Stem Cell Technologies, Vancouver, BC), as described (MacGlashan et al. 1994). Basophils counts and purities were determined by staining with Alcian blue (Pruzansky et al. 1983) and generally exceeded 99% purity.

Eosinophils. Eosinophils were isolated from allergic donors on a Johns Hopkins Institutional Review Board approved clinical protocol (NA 00036470) following written informed consent using density gradient centrifugation, hypotonic lysis of erythrocytes and immunomagnetic depletion of neutrophils with CD16 mAb and magnetic beads as described previously (Matsumoto et al. 1997).

Mast cells. CD34+ cells were obtained from unidentified blood donors or normal or allergic volunteers on an NIAID Institutional Review Board approved clinical protocol (NIH 98-I-0027) following written informed consent and with or without granulocyte colony-stimulating factor before leukapheresis, followed by a positive selection as described (Kirshenbaum et al. 1999; Kulka and Metcalfe 2005; Yokoi et al. 2006).

Human mast cells were derived by culture of these CD34+ peripheral blood precursors, as described (Kirshenbaum et al. 1999; Yokoi et al. 2006). Briefly, cells were cultured at a starting concentration of 5×10^5 cells/mL in serum-free medium (StemPro-34 SFM; Life Technologies, Grand Island, NY) supplemented with 2 mM L-glutamine, 100 IU/mL penicillin, 50 µg/mL streptomycin, 100 ng/mL recombinant human SCF (Biosource, Camarillo, CA), 100 ng/mL recombinant human IL-6 (Biosource) and 30 ng/mL recombinant human IL-3 (R&D Systems, Minneapolis, MN), the latter for the first week only. Hemi-depletions of media were performed weekly, replacing this with fresh media containing 100 ng/mL SCF and 100 ng/mL IL-6. Cells were cultured at 37°C with 5% CO_2. Cell counts and viability were checked each week by Trypan blue staining. Mast cells were used after 10.5 weeks of culture. LAD2 cells were maintained in serum-free media with SCF (100 ng/mL; Kirshenbaum et al. 2003).

Aliquots of mast cells were activated for 6 h at 37°C by aggregation of FcRI using the anti-Fc α-chain antibody CRA-1 at 1 µg/mL (IgG1 mouse anti-human Fc α-chain from eBioscience, San Diego, CA).

Preparation of cells for glycomic analyses

Cells were resuspended in 1 mL of phosphate-buffered saline, transferred to a microfuge tube and pelleted at 800*g*. The supernatant was aspirated and the cell pellet was stored at −80°C.

Reduction and carboxymethylation

Each cell sample (~10×10^7 eosinophils, 15×10^6 mast cells and 10^6 basophils) was sonicated in extraction buffer (25 mM Tris, 150 mM NaCl, 5 mM ethylenediaminetetraacetic acid (EDTA) and 1% 3-[(3-cholamidopropyl)dimethylammonio]-1-propanesulfonate (CHAPS) at pH 7.4) and then dialyzed against 4 × 4.5 L of 50 mM ammonium bicarbonate, pH 8.5,

at 4°C for 48 h as described (Sutton-Smith and Dell 2006). After dialysis, the sample was lyophilized and then reduced in 1 mL of 50 mM Tris–HCl buffer, pH 8.5, containing 2 mg/mL of dithiothreitol. Reduction was performed under a nitrogen atmosphere at 37°C for 1 h. Carboxymethylation was carried out by the addition of iodoacetic acid (5-fold molar excess over dithiothreitol), and the reaction was allowed to proceed under a nitrogen atmosphere at room temperature in the dark for 2 h. Carboxymethylation was terminated by dialysis against 4 × 4.5 L of 50 mM ammonium bicarbonate, pH 8.5, at 4°C for 48 h. After dialysis, the sample was lyophilized.

Tryptic digest

The reduced carboxymethylated proteins were digested with tosyl phenylalanyl chloromethyl ketone (TPCK) pretreated bovine pancreas trypsin (EC3.4.21.4, Sigma-Aldrich, Dorset, UK), for 16 h at 37°C in 50 mM ammonium bicarbonate buffer (pH 8.4). The products were purified by C_{18}-Sep-Pak (Waters Corp., Elstree, UK) as described (Dell et al. 1994).

Sep-Pak® separation of released glycans from peptides

The reverse-phase C_{18} Sep-Pak cartridge was primed sequentially with 5 mL of methanol, 5 mL of 5% acetic acid (v/v) and 5 mL of propan-1-ol before being re-equilibrated with 10 mL of 5% acetic acid (v/v). The sample was then dissolved in a minimum volume of 5% acetic acid (v/v) and loaded directly onto the Sep-Pak. Elution was achieved using 3 mL of 5% acetic acid (v/v), followed by 2 mL each of 20, 40, 60 and 100% propan-1-ol in 5% acetic acid (v/v). Each elution step was collected, reduced in volume on a Speed Vac and lyophilized (Dell et al. 1994).

PNGase F digestion of glycopeptides

PNGase F (EC3.5.1.52, Roche Molecular Biochemicals, Lewes, UK) digestion was carried out in 200 µL of ammonium bicarbonate (50 mM, pH 8.5) for 16 h at 37°C using 3 U of enzyme. The reaction was terminated by lyophilization and the released *N*-glycans were separated from peptides and O-glycopeptides by Sep-Pak C_{18} (Waters Corp.) as described (Dell et al. 1994).

Sep-Pak® separation of permethylated glycans

The reverse-phase C_{18} Sep-Pak cartridge was primed sequentially with 5 mL methanol, 5 mL water and 5 mL acetonitrile before being re-equilibrated with 10 mL of water. The lyophilized permethylated oligosaccharide sample was then dissolved in a minimum volume of methanol and loaded directly onto the Sep–Pak. Elution was achieved using 3 mL of water followed by 2 mL each of 15, 30, 50, 75 and 100% acetonitrile in water (v/v). Each elution step was collected, reduced in volume on a Speed Vac and lyophilized (Dell et al. 1994).

Derivatization for MALDI-TOF and tandem MS analysis

Permethylation was performed using the sodium hydroxide procedure, as described (Dell et al. 1994). One gram of sodium hydroxide pellets was crushed in a glass mortar with 3 mL of distilled, anhydrous dimethyl sulfoxide (DMSO). One milliliter of the resulting slurry and 200 µL of methyl iodide were added to the lyophilized sample. The mixture was then shaken for 10 min before the reaction was quenched by dropwise addition of water. The permethylated sample was next extracted into 1 mL of chloroform and washed with 4 × 1 mL of water. The chloroform was then removed under a stream of nitrogen.

Partially methylated alditol acetates were prepared from permethylated samples for GC-MS linkage analysis as described (Albersheim et al. 1967). The permethylated glycans were hydrolyzed with 2 M trifluoroacetic acid for 2 h at 121°C, reduced with 10 mg/mL of sodium borodeuteride in 2 M aqueous ammonium hydroxide at room temperature for 2 h, then acetylated with acetic anhydride at 100°C for 1 h.

Mass spectrometric analysis

MALDI-TOF data were acquired on a Voyager-DE STR mass spectrometer (Applied Biosystems, Foster City, CA) in the reflectron mode with delayed extraction. Permethylated samples were dissolved in 10 µL of 80% (v/v) aqueous methanol and 1 µL of dissolved sample was premixed with 1 µL of matrix [20 mg/mL of 2,5-dihydroxybenzoic acid in 80% (v/v) aqueous methanol], spotted onto a target plate and dried under vacuum. Further MS/MS analyses of peaks observed in the MS spectra were carried out using a 4800 MALDI-TOF/TOF (Applied Biosystems) mass spectrometer. The potential difference between the source acceleration voltage and the collision cell was set to 1 kV and argon was used as collision gas. The 4700 Calibration Standard Kit, calmix (Applied Biosystems), was used as the external calibrant for the MS mode and [Glu^1] fibrinopeptide B human (Sigma-Aldrich) was used as an external calibrant for the MS/MS mode. Data from the MALDI-MS glycomic experiments are available in the CFG databases (http://www.functionalglycomics.org/glycomics/publicdata/glycoprofiling-new.jsp).

GC-MS linkage analysis

GC-MS linkage analysis of partially methylated alditol acetates were carried out using a Perkin Elmer Clarus 500 instrument (PerkinElmer, Cambridgeshire, UK) fitted with a RTX-5 fused silica capillary column (30 m × 0.32 mm internal diameter, Restek Corp., PA). The sample was dissolved in hexanes and injected onto the column at 60°C. The column was maintained at this temperature for 1 min and then heated to 300°C at a rate of 8°C/min.

Automated MS and MS/MS analysis

Annotation of the MS and MS/MS data was achieved with assistance from the Cartoonist algorithm (Goldberg et al. 2005) and the GlycoWorkbench software suite (Ceroni et al. 2008).

Funding

This work was supported by the Analytical Glycotechnology Core (Core C) of the Consortium for Functional Glycomics (GM 62116), the Swiss National Foundation (PBBEB-113394 to S.G.), the National Institutes of Health (AI 72265 to B.S.B.)

and by the National Institute of Allergy and Infectious Diseases Division of Intramural Research.

Conflict of interest

None declared.

Abbreviations

CFG, Consortium for Functional Glycomics; CHAPS, 3-[(3-cholamidopropyl)dimethylammonio]-1-propanesulfonate; ConA, concanavalin A; DMSO, dimethyl sulfoxide; EDTA, ethylenediaminetetraacetic acid; e-PHA, phaseolus vulgaris lectin E; Fuc, fucose; Gal, galactose; GC, gas chromatography; GlcNAc, *N*-acetylglucosamine; Hex, hexose; HexNAc, *N*-acetylhexosamine; ITIM, immunoreceptor tyrosine-based inhibitory motif; LacNAc, Galβ1-4GlcNAc; LAD, leukocyte adhesion deficiency; LCA, lens culimaris agglutinin; l-PHA, phaseolus vulgaris lectin L; Man, mannose; MALDI, matrix-assisted laser desorption ionization; MS, mass spectrometry; NeuAc, *N*-acetylneuraminic acid; PNGase F, peptide *N*-glycosidase F; PSA, Pisum sativum agglutinin; SCF, stem cell factor; siglec, sialic acid-binding immunoglobulin-like lectin; TOF, time of flight; TPCK, tosyl phenylalanyl chloromethyl ketone; WGA, wheat germ agglutinin.

References

Agis H, Fureder W, Bankl HC, Kundi M, Sperr WR, Willheim M, Boltz-Nitulescu G, Butterfield JH, Kishi K, Lechner K, et al. 1996. Comparative immunophenotypic analysis of human mast cells, blood basophils and monocytes. *Immunology*. 87:535–543.

Albersheim P, Nevins DJ, English PD, Karr A. 1967. A method for the analysis of sugars in plant cell-wall polysaccharides by gas-liquid chromatography. *Carbohydr Res*. 5:340–345.

Avril T, North SJ, Haslam SM, Willison HJ, Crocker PR. 2006. Probing the *cis* interactions of the inhibitory receptor Siglec-7 with α2,8-disialylated ligands on natural killer cells and other leukocytes using glycan-specific antibodies and by analysis of α2,8-sialyltransferase gene expression. *J Leukoc Biol*. 80:787–796.

Babu P, North SJ, Jang-Lee J, Chalabi S, Mackerness K, Stowell SR, Cummings RD, Rankin S, Dell A, Haslam SM. 2009. Structural characterisation of neutrophil glycans by ultra sensitive mass spectrometric glycomics methodology. *Glycoconj J*. 26:975–986.

Bax M, Garcia-Vallejo JJ, Jang-Lee J, North SJ, Gilmartin TJ, Hernandez G, Crocker PR, Leffler H, Head SR, Haslam SM, et al. 2007. Dendritic cell maturation results in pronounced changes in glycan expression affecting recognition by siglecs and galectins. *J Immunol*. 179:8216–8224.

Bochner BS, Schleimer RP. 2001. Mast cells, basophils, and eosinophils: Distinct but overlapping pathways for recruitment. *Immunol Rev*. 179:5–15.

Canis K, McKinnon TA, Nowak A, Panico M, Morris HR, Laffan M, Dell A. 2010. The plasma von Willebrand factor O-glycome comprises a surprising variety of structures including ABH antigens and disialosyl motifs. *J Thromb Haemost*. 8:137–145.

Ceroni A, Maass K, Geyer H, Geyer R, Dell A, Haslam SM. 2008. GlycoWorkbench: A tool for the computer-assisted annotation of mass spectra of glycans. *J Proteome Res*. 7:1650–1659.

Crocker PR, Paulson JC, Varki A. 2007. Siglecs and their roles in the immune system. *Nat Rev Immunol*. 7:255–266.

Dell A, Reason AJ, Khoo KH, Panico M, McDowell RA, Morris HR. 1994. Mass spectrometry of carbohydrate-containing biopolymers. *Methods Enzymol*. 230:108–132.

Dominguez-Soto A, Aragoneses-Fenoll L, Martin-Gayo E, Martinez-Prats L, Colmenares M, Naranjo-Gomez M, Borras FE, Munoz P, Zubiaur M, Toribio ML, et al. 2007. The DC-SIGN-related lectin LSECtin mediates antigen capture and pathogen binding by human myeloid cells. *Blood*. 109:5337–5345.

Fukuda M, Lauffenburger M, Sasaki H, Rogers ME, Dell A. 1987. Structures of novel sialylated O-linked oligosaccharides isolated from human erythrocyte glycophorins. *J Biol Chem*. 262:11952–11957.

Goldberg D, Sutton-Smith M, Paulson J, Dell A. 2005. Automatic annotation of matrix-assisted laser desorption/ionization *N*-glycan spectra. *Proteomics*. 5:865–875.

Kirshenbaum AS, Akin C, Wu Y, Rottem M, Goff JP, Beaven MA, Rao VK, Metcalfe DD. 2003. Characterization of novel stem cell factor responsive human mast cell lines LAD 1 and 2 established from a patient with mast cell sarcoma/leukemia; activation following aggregation of FcRI or FcγRI. *Leuk Res*. 27:677–682.

Kirshenbaum AS, Goff JP, Semere T, Foster B, Scott LM, Metcalfe DD. 1999. Demonstration that human mast cells arise from a progenitor cell population that is CD34(+), c-kit(+), and expresses aminopeptidase N (CD13). *Blood*. 94:2333–2342.

Kulka M, Metcalfe DD. 2005. High-resolution tracking of cell division demonstrates differential effects of TH1 and TH2 cytokines on SCF-dependent human mast cell production in vitro: Correlation with apoptosis and kit expression. *Blood*. 105:592–599.

Lee CG, Elias JA. 2010. Role of breast regression protein-39/YKL-40 in asthma and allergic responses. *Allergy Asthma Immunol Res*. 2:20–27.

Lee CG, Hartl D, Lee GR, Koller B, Matsuura H, Da Silva CA, Sohn MH, Cohn L, Homer RJ, Kozhich AA, et al. 2009. Role of breast regression protein 39 (BRP-39)/chitinase 3-like-1 in Th2 and IL-13-induced tissue responses and apoptosis. *J Exp Med*. 206:1149–1166.

MacGlashan DW, Jr., Bochner BS, Warner JA. 1994. Graded changes in the response of individual human basophils to stimulation: Distributional behavior of early activation events. *J Leukoc Biol*. 55:13–23.

Matsumoto K, Sterbinsky SA, Bickel CA, Zhou DW, Kovach NL, Bochner BS. 1997. Regulation of α4 integrin-mediated adhesion of human eosinophils to fibronectin and vascular cell adhesion molecule-1 (VCAM-1). *J Allergy Clin Immunol*. 99:648–656.

Matsuura H, Hartl D, Kang MJ, Dela Cruz CS, Koller B, Chupp GL, Homer RJ, Zhou Y, Cho WK, Elias JA, et al. 2011. Role of Breast Regression Protein (BRP)-39 in the Pathogenesis of Cigarette Smoke-Induced Inflammation and Emphysema. *Am J Respir Cell Mol Biol*. 44:777–786.

Miyazaki S, Sugawara H, Tamura T, Okayama T, Ishii J, Shimura J, Yoshida K, Saijo K, Ohno T, Blanchard D, et al. 1997. Cross-lineage (Blind Panel) study and human leucocyte differentiation antigen database. In: Kishimoto T, Kikutani H, von dem Borne AEGK, Goyert SM, Mason DY, Miyasaka M, Moretta L, Okumura K, Shaw S, Springer TA, et al., editors. *Leucocyte Typing VI: White Cell Differentiation Antigens*. New York: Garland Publishing, Inc. p. 3–20.

Nakajima T, Matsumoto K, Suto H, Tanaka K, Ebisawa M, Tomita H, Yuki K, Katsunuma T, Akasawa A, Hashida R, et al. 2001. Gene expression screening of human mast cells and eosinophils using high-density oligonucleotide probe arrays: Abundant expression of major basic protein in mast cells. *Blood*. 98:1127–1134.

Ober C, Chupp GL. 2009. The chitinase and chitinase-like proteins: A review of genetic and functional studies in asthma and immune-mediated diseases. *Curr Opin Allergy Clin Immunol*. 9:401–408.

O'Reilly MK, Paulson JC. 2009. Siglecs as targets for therapy in immune-cell-mediated disease. *Trends Pharmacol Sci*. 30:240–248.

Perdivara I, Petrovich R, Allinquant B, Deterding LJ, Tomer KB, Przybylski M. 2009. Elucidation of O-glycosylation structures of the beta-amyloid precursor protein by liquid chromatography-mass spectrometry using electron transfer dissociation and collision induced dissociation. *J Proteome Res*. 8:631–642.

Powlesland AS, Fisch T, Taylor ME, Smith DF, Tissot B, Dell A, Pohlmann S, Drickamer K. 2008. A novel mechanism for LSECtin binding to Ebola virus surface glycoprotein through truncated glycans. *J Biol Chem*. 283:593–602.

Pruzansky JJ, Grammer LC, Patterson R, Roberts M. 1983. Dissociation of IgE from receptors on human basophils. I. Enhanced passive sensitization for histamine release. *J Immunol*. 131:1949–1953.

Roberts IS, Jones CJ, Stoddart RW. 1990. Lectin histochemistry of the mast cell: Heterogeneity of rodent and human mast cell populations. *Histochem J*. 22:73–80.

Sutton-Smith M, Dell A. 2006. Analysis of carbohydrates/glycoproteins by mass spectrometry. In: Celis JE, editor. *Cell Biology: A Laboratory Handbook*. San Diego (CA): Academic Press. p. 425–435.

Tang L, Yang J, Liu W, Tang X, Chen J, Zhao D, Wang M, Xu F, Lu Y, Liu B, et al. 2009. Liver sinusoidal endothelial cell lectin, LSECtin, negatively regulates hepatic T-cell immune response. *Gastroenterology.* 137:1498–1508.e1491–e1495.

Valent P. 1994. The phenotype of human eosinophils, basophils, and mast cells. *J Allergy Clin Immunol*. 94:1177–1183.

Varki A, Cummings RD, Esko JD, Freeze HH, Stanley P, Marth JD, Bertozzi CR, Hart GW, Etzler ME. 2009. Symbol nomenclature for glycan representation. *Proteomics*. 9:5398–5399.

Wada Y, Azadi P, Costello CE, Dell A, Dwek RA, Geyer H, Geyer R, Kakehi K, Karlsson NG, Kato K, et al. 2007. Comparison of the methods for profiling glycoprotein glycans—HUPO Human Disease Glycomics/Proteome Initiative multi-institutional study. *Glycobiology.* 17:411–422.

Yabe R, Tateno H, Hirabayashi J. 2010. Frontal affinity chromatography analysis of constructs of DC-SIGN, DC-SIGNR and LSECtin extend evidence for affinity to agalactosylated N-glycans. *FEBS J.* 277:4010–4026.

Yasukawa Z, Sato C, Sano K, Ogawa H, Kitajima K. 2006. Identification of disialic acid-containing glycoproteins in mouse serum: A novel modification of immunoglobulin light chains, vitronectin, and plasminogen. *Glycobiology.* 16:651–665.

Yokoi H, Myers A, Matsumoto K, Crocker PR, Saito H, Bochner BS. 2006. Alteration and acquisition of Siglecs during *in vitro* maturation of CD34+ progenitors into human mast cells. *Allergy.* 61:769–776.